IEEE Access
Multidisciplinary ⋮ Rapid Review ⋮ Open Access Journal

Received 20 May 2024, accepted 30 May 2024, date of publication 6 June 2024, date of current version 13 June 2024.

Digital Object Identifier 10.1109/ACCESS.2024.3410374

RESEARCH ARTICLE

A New Method of Smart Control of Single-Phase Photovoltaic Inverters at Low Voltage for Voltage Control and Reactive Power Management

JOSEF HROUDA[1], MARTIN ČERŇAN[2], (Member, IEEE), AND KAREL PROCHÁZKA[3]
[1]Department of Power Engineering, Faculty of Electrical Engineering, University of West Bohemia, 301 00 Pilsen, Czech Republic
[2]Department of Electrical Power Engineering, Faculty of Electrical Engineering, Czech Technical University in Prague, 166 36 Prague, Czech Republic
[3]EGC—EnerGoConsult ČB s.r.o., 370 01 České Budějovice, Czech Republic

Corresponding author: Josef Hrouda (jhrouda@egc-cb.cz)

This work was supported in part by the EGC—EnerGoConsult ČB s.r.o., and in part by Czech Technical University in Prague under Grant SGS23/167/OHK3/3T/13.

ABSTRACT This paper introduces a newly designed reactive power control method for single-phase photovoltaic (PV) inverters. The control focuses on easy application and autonomous actions. The regulation is designed with regard to the effective network operation and the saving of reactive power with the functionality of voltage control and optimization of active losses. This paper proves the easy application of the newly proposed control design using the implementation of a control algorithm into a dynamic photovoltaic power plant (PVP) model and supply point with PSCAD software. The long-term benefit of this control is illustrated by the MATLAB/Simulink case study of a one-week simulation over the CIGRE LV European benchmark four-wire network using data from smart meters and measured PVP generation, which was provided by the Distribution System Operator (DSO). The case study showed the benefits of the newly designed regulation in terms of saving reactive energy supply from the upstream system by up to 64% (the regulation contributes to the self-sufficiency of the LV network in terms of reactive power), a positive effect on the reduction of active losses by up to 1.5% and a simultaneous improvement of the voltage profile at the nodes of the modelled network is also observed. The case study also reveals the risks of autonomous control of $Q = f(V)$ single phase inverter on the voltage unbalance depending on its definition.

INDEX TERMS LV grid, PVP, reactive power management, single phase inverter, voltage control, voltage unbalance.

NOMENCLATURE

DC	Direct current.
DG	Distributed generation.
DN	Distribution network.
DSO	Distribution system operator.
EMTDC	Electromagnetic transients including direct current.
EU	European Union.
LAN	Local area network.
LV	Low voltage.
MPPT	Maximum power point tracker.
MV	Medium voltage.
OLTC	On-load tap changing transformer.
OPF	Optimal power flow.
PV	Photovoltaic.
PVP	Photovoltaic power plant.
PWM	Pulse-width modulation.
RfG	Requirements for Generators.
UK	United Kingdom.

The associate editor coordinating the review of this manuscript and approving it for publication was Fabio Mottola.

I. INTRODUCTION

A. MOTIVATION

Planned and gradually progressing decay of conventional power sources, increasing penetration of DG in the power mix [1], [2], the moving of sources to the MV and LV DN together with the continuing trend of replacing overhead lines with cables in MV and LV networks creates the need for reliable and effective management of reactive power across the different voltage levels of the power system [3], [4]. The reactive power is utilized for massive penetration of DG into lower voltage DN [5], [6], [7]. Regarding DN operation, the reactive power is mostly associated with voltage magnitude (despite the unfavorable R / X ratio for voltage regulation by reactive power at the LV level) and additional technical losses, resulting from the required reactive power of DG [8]. Additionally, the voltage unbalance is experienced at LV due to the mix of non-symmetrical loads and power generation [9]. Voltage unbalance is an ever more important topic, particularly because of the increasing penetration of PVP, including PVP with single-phase connection [9] as well as e-vehicle charging stations [10], [11]. Their impact on the network can be significant, particularly when LV terminal impedance is similar or higher [12] than reference impedances that are defined in IEC 61000-3-3 [9].

The newly developed control algorithm responds to the small effect of reactive power control on the magnitude of the voltage at the LV level. Therefore, it uses the autonomous control characteristic $Q = f(V)$ only as a safety brake for the voltage. The wide range of insensitivity of the $Q = f(V)$ control is used for the reactive power management of the load point, where the inverter control potential in the reactive power region compensates the reactive power consumption of the load points. This makes the LV network more self-sufficient in terms of reactive power. This contributes to the reduction of active losses in the transmission and distribution of electricity. The compensated load points in each phase contribute to the current symmetry of the load. The newly designed control aims at easy applicability and local character of the control.

B. DG AND PVP - EXISTING STATUS AND PERSPECTIVE

Distributed Generation (DG) development in Europe was accelerated mainly by the European Green Deal [1]. Photovoltaic power plants (PVP) in this plan represent a significant and frequently installed DG. The existing situation regarding the installed PVP power in European countries is described in [13]. The highest ratio of PVP generation can be found in Germany (58 GW in 2022) followed by the Netherlands (16 GW) and Spain (15 GW).

Yet additional DG development (especially PVP) in the mid-term horizon for member states, particularly in Germany, Spain and France until 2030, is predicted in documents [14] and [15]. According to [14], there is an ever-increasing portion of rooftop PVP, which represents more than 60% of installed PVP power. These rooftop installations cover about 15% (based on [14]) of identified roof potential in the EU and UK. Therefore, the utilization of the whole potential for rooftop PVP in the EU and UK represents 540 GW of installed power. In general, residential rooftop PVP present small power generation that is connected to the LV level. Based on installed power and utilization (household consumption, combination with power storage, optional injection of surplus power into the network), they can use single-phase or three-phase connection.

Development prediction for PVP inverters can be found in many business research reports published by commercial utilities for the EU, North America and Asia-Pacific regions. The market report [16] distinguishes the three-phase inverters in its prediction. Contrary, market report [17] predicts the residential and small commerce sector as the one with the fastest development. Hence, it identifies the single-phase inverters for small applications as the fastest-developing technology of the PVP inverters. This development is acknowledged by market report [18] as well. Therefore, this paper and research focus on single-phase PVP inverters for household rooftops application.

C. REQUIREMENTS FOR NEWLY CONNECTED PVP INVERTER CONTROL

The key document defining the requirements for newly connected generation in the EU is RfG issued in 2016 [5]. RfG code is implemented by national legislation. These requirements can be toughened up on the national level. Sources connected to the LV level shall comply with standard EN 50549-1 [7]. Implementation of RfG requirements into national legislation was digestedly described in [19]. Table 1 shows the list of member states in which national requirements for Type A (connection point below 110 kV and a maximum power of 0.8–999 kW according to RfG) sources are stricter than those defined by RfG. Most of the other member states implemented requirements as defined by RfG.

With the increase of installed power of small generation at the LV level, the tightening up of reactive power control can be expected even for Type A generation. Single-phase connection is usually limited in terms of maximum power by national legislation, which in member states of the EU is usually in the range of 3.68–5.0 kW/phase [20] (4.6 kVA/phase in Germany [21], which has the highest installed photovoltaic power plant (PVP) power within the EU, while only 3.68 kW/phase in the Czech Republic [22], which is the most common limit in the EU). The highest power limit for a single phase can be found in France (6 kW/phase) [20].

D. TYPICAL CONFIGURATION OF SINGLE-PHASE PVP ACCORDING TO EXISTING LEGISLATION

The primary task of rooftop photovoltaic power plant (PVP) is financial profit for the plant owner, the inverter provides minimum support for the LV network only [5], [7], [19], which is in compliance with national legislation valid in the year of commissioning. The owner's financial profit principle

TABLE 1. Specific auxiliary functions, comparison of RfG for Type A generation and EN 50549-1 [7] with national legislation of specific member states and UK; source [19].

	RfG	EN 50549-1	Germany	Italy	Austria
Type A power limit (MW)	≤1	≤1	≤0.135	≤0.011	≤0.25
$P=f(f)$	No	Yes	Yes	Yes	No
Q / cos φ range	No	Yes	Yes (cos φ)	Yes (all)	Yes
cos $\varphi = f(P)$	No	Yes	Yes	Yes	Yes
$Q=f(V)$	No	Yes	>4.6 kVA	>11.08 kW*	Yes
$P=f(V)$	No	Optional	Allowed	Optional	Yes
Ramp rate limits	No	No	Yes	No	No
Remote control of P	No	Yes	>30 kW	>11.08	No
Remote control of Q	No	Optional	No	>11.08	No
LVRT	No	Yes	Yes*	>11.08	Yes
HVRT	No	Yes	Yes*	No	No
Fast reactive current		No	No	No	No/Yes*
NOTE			* Not required	* Additional lock-in/- out function	* On request of DSO

may vary according to the connection agreement based on the support schemes of each state. Support schemes of EU member states are depicted in [23].

In the case of single-phase inverters, the consumption of the supply point and PVP are usually connected to the same phase. In EU member states, small PVP installations participate usually in network support in terms of unified frequency behavior during significant frequency variations. The $Q=f(V)$ control and the $P=f(V)$ controls are required in some EU member states. The $P=f(V)$ control is utilized as an emergency brake if reactive power control potential is depleted. Active power is decreased usually for limit voltage values, e.g. $V/V_n = 1.09$. Hence, there is no harmonized control of reactive power at the supply point. Reactive power flow can be indirectly controlled by $Q=f(V)$. Since these control functions are autonomous and since LV networks can be supplied by OLTC transformers, the setting of these control measures shall be well harmonized [24]. The PQ diagram that is provided by the manufacturer shows the generation control options and potential of sources. The reactive power control range must comply with minimum requirements defined by national legislation.

E. LITERATURE OVERVIEW

Existing scientific and research projects that deal with single-phase inverter control at the LV level or other solutions have shown the efforts for voltage control in LV networks, improving voltage unbalance, and increasing the effectiveness of LV networks.

Simple voltage control in the LV network can be achieved by OLTC transformers. The voltage control system of an OLTC transformer can vary from voltage control on the busbar only to communication coupling to the voltage critical point in networks [24], [25], [26]. LV networks with high DG penetration can experience frequent tap changing. According to [27], there is an approach to harmonize PVP inverter control by smoothing the change in apparent PVP power so that frequent tap changing can be avoided. A positive impact on voltage management of this type of control either with or without OLTC transformers is demonstrated in [28], [29], [30], and [31], but the necessity of a very well harmonized control setting with network as well as other control elements is emphasized.

The comparison of the autonomous control functions of inverters that are implemented in firmware today is analyzed in detail in paper [31]. The results over the reference network show the benefits of inverter control in favor of voltage. This helps to increase the Hosting Capacity. The possible consequences of increased active losses due to reactive power regulation are mentioned as well as the necessary good coordination of autonomous regulation. Finally, the necessity of developing new ways of controlling LV inverters and networks is discussed.

Sophisticated network control solutions using inverters and other actuators as described in [32], [33], [34], and [35] utilize a wide range of communication measures within the LV network to optimize the network operation. These solutions often utilize data from smart metering [36], [37]. Smart meters may in general provide aggregated and/or real-time data for control [38]. These solutions, based on OPF with central computational logic, demonstrate good results in optimizing voltage, losses and voltage asymmetry at the cost of a large communication network and interoperability.

An effective method of LV network operation improvement is to incentivize prosumers to achieve flexibility of load and generation. Financial incentives may be offered to provide flexibility for the network, as demonstrated in [39].

Regarding the voltage unbalance and magnitude, asymmetrical inverters present an effective solution [32]. Yet, such equipment is significantly more expensive for PVP use than a simple single-phase inverter.

An interesting approach is provided in [28], where inverter control is location dependent. Hence, inverter control can be properly set and selected based on the impedance in the supply point. Nevertheless, such an approach required the harmonization of connection and network analysis. Article [40] presents modified conventional control for the single-phase inverter power factor but in steps defined by the voltage. The benefits regarding the voltage magnitude and voltage unbalance are described. However, voltage unbalance was calculated using a simplified definition that does not consider voltage angles. Therefore, the presented voltage

unbalance improvement achieved by reactive power control in a single phase can be misleading.

Other presented schemes demonstrate the benefits of the installation of DSO owned external compensation equipment improving voltage profile [41], [42]. Additionally, [42] recommends prosumer independence regarding the reactive power (autarkic) together with external DSO compensation using inductances as one of the best options for LV network operation within the accomplished analysis. The inverter thus works in the role of a compensator.

Other works also deal with the inverter as a compensator. Article [43] presents the PV inverter as a load current compensator with a sliding mode controller current control loop. The inverter is also used as a reactive power compensator when solar illumination is not available. For these cases, a control loop is additionally applied to control the voltage in the DC circuit. The presented approach significantly improves the power factor of the network and the overall harmonic distortion. Article [44] again uses the PV inverter as a reactive power compensator. To ensure that the inverter has developed sufficient control potential, an MPPT method is presented to create a margin for the wide application of reactive power control in current sizing. These are alternatives in order to create inverter control potential without oversizing the device and having to install additional reactive power compensation devices.

Reference [45] uses switching inductive elements for voltage control purposes and inverters as reactive power compensators for appliances. When there is significant generation from PV, inductances owned by the DSO are switched. This method of regulation is known as $L(V)$ control. The results of the study show that the deployment of inverters as compensators in combination with $L(V)$ control achieves a stable voltage profile, reduction of reactive power flows as well as reduction of active losses. The limitation of reactive power flows in LV networks brings an increase in Hosting Capacity.

Article [46] presents the inverter as a compensator for voltage. Innovative strategies for adjusting the autonomous characteristic $Q = f(V)$ to make the reactive power redistribution fair are presented. The strategies described in this way use communication between master and slave inverters. The issue of using inverter oversizing to benefit the control potential and cooperation with STATCOM systems is also addressed. Reference [47] provides a comparison of reactive power management of LV level inverters. The functions compared were $Q = f(V)$, constant power factor, power factor adjustment according to schedule and power factor adjustment in defined steps. The paper evaluates the positive contribution of all methods of inverter control on voltage and in conclusion the authors point out the necessity of applying economic control principles with respect to the amount of control reactive power and active losses. A possible solution to the previous conclusion is given in reference [48]. The authors implemented the standard $Q = f(V)$ control. If the voltage measured by the inverter is in the insensitivity band, the central logic can command the inverter to control in another way, for example as a reactive power compensator. However, this control method requires communication links to the central logic of the network.

Inverter manufacturers provide the Q 24/7 function (reactive power compensation) to achieve reactive power self-sustainability. The utilization of such function to support the network is dealt with in [49], [50], [51], and [52].

Implementations of control loops in terms of their effectiveness on control quality (dynamics, harmonic content, etc.) are discussed in the literature [53] and [54].

F. PAPER ORGANISATION

This paper is divided into seven sections. Section I. describes the reasoning for the selected topic of new control of single-phase PVP at the LV level. The legislative frame of European countries is introduced as well as the typical configuration of single-phase PVP systems from an LV DN point of view. The last part of this section deals with research on existing and innovative methods of LV network control in available publications.

Section II. presents in detail a newly designed control algorithm for a single-phase inverter. Additionally, it contains the derivation of the principle for the newly developed control algorithm for single-phase inverters, which incorporates the future needs of network operation specified in the first section and the first part of the second section.

Section III. describes the implementation of the newly developed control into a dynamic PVP model using PSCAD software and the presentation of results of dynamic simulations in regard to existing legislation.

Section IV. introduces the newly developed control case study of long-term benefits that are based on the four-wire benchmark CIGRE European LV distribution network created in MATLAB/Simulink.

Section V. presents the results of the case study including a comparison of each LV network setting based on the evaluation criteria (voltage, voltage unbalance, active power losses and overall reactive power energy in the modelled network).

Section VI. contains the conclusion and Section VII. contains recommendations for future work.

II. HYPOTHESIS - POSSIBLE IMPROVEMENTS OF LV NETWORK CONTROL FOCUSING ON SINGLE-PHASE INVERTERS

A. DERIVATION OF A NEWLY DESIGNED CONTROL ALGORITHM FOR A SINGLE-PHASE PV INVERTER

Control and optimization of LV networks should aim for safe operation, so the limits defined by [55] are not exceeded as well as control effectivity to avoid unnecessary increase of active power losses. Due to the above-mentioned increase in the installed capacity of PVP, usually single-phase connected, the suitable control in the LV network targets voltage magnitude, unbalance optimization and minimizing reactive power flows and the active power losses. Since the primary

focus of PVP household sources is to generate profit and fast return on investment, any network support that is not mandatory according to the legislation is hardly applicable. Moreover, reactive power control results in thermal load of inverter elements (particularly DC capacitor) [50], which may decrease its service life [56]. Therefore, the newly designed control focuses primarily on the inverter's mandatory network support using reactive power, while active power is not affected. Should such control (e.g. by "Q on Demand", alternatively called "Q at night" or Q 24/7) be outside the mandatory network support, the legislative framework for the LV level needs to be introduced to incentivize householders (see [39]).

The references of photovoltaic (PV) inverters in the role of voltage compensators show the risk of their low efficiency at the LV level and the possible increase of active losses during significant flows of control reactive power [31], [46]. A more effective use is then brought by the role of inverters as compensators for reactive power at the LV level [48]. The newly designed control tries to consider the supply point together with PVP installation as a reactive power control element. Regarding the local impact of the reactive power control, this control is autonomous in relation to the supply point and unlike approaches described in [27], [32], [33], [34], and [48], there is no communication with the central network logic or other points of connection, which saves additional costs of installation and general control implementation.

The LV network impedance can be defined through R/X ratio, which for the LV network should be in the range of 0.7 and 11 [57]. The value of R/X ratio increases with distance from the supply transformer [8]. The voltage drop on the network impedance is expressed by (1).

$$\Delta V = (R + jX)\left(I_{real} \pm jI_{imaginary}\right) \tag{1}$$

where ΔV is a voltage change in V, R is network resistance in Ω, X is a network reactance in Ω, I_{real} is a real component of network current in A and $I_{imaginary}$ is an imaginary component of network current in A. By expressing active and reactive power and by omitting imaginary components, (1) can be expressed as follows (2).

$$\Delta V = \frac{(RP \pm XQ)}{3V} \tag{2}$$

where P is active power in kW, Q is reactive power in kVAr and V is a voltage in V. The voltage change ratio between the case when the plant does and does not control the reactive power is expressed by (3).

$$c = \frac{\Delta V_{\cos\varphi \neq 1}}{\Delta V_{\cos\varphi = 1}} \tag{3}$$

where c is a dimensionless factor of voltage change, $\Delta V_{\cos\varphi \neq 1}$ is a voltage change in V of a plant with reactive power control and $\Delta V_{\cos\varphi = 1}$ is a voltage change in V of a plant without the reactive power control. Using above-mentioned (2) and (3) we can derive:

$$c \cong \frac{RP \pm XQ}{RP} \tag{4}$$

$$\frac{RP \pm XQ}{RP} = 1 \pm \frac{X}{R} \cdot \frac{Q}{P} \tag{5}$$

Fig. 1 shows the impact of R/X on the magnitude of voltage change caused by reactive power control.

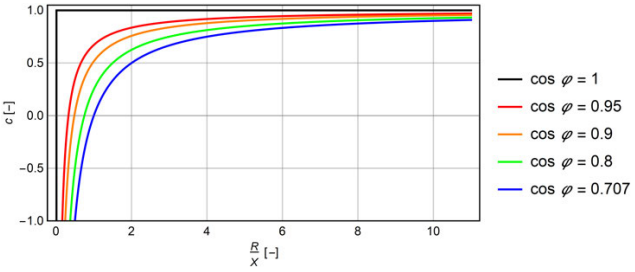

FIGURE 1. The impact of voltage changes during the reactive power control on *R / X* impedance in the supply point.

As was mentioned, for the LV network, R / X is usually in the range of 0.7 and 11 [57]. This value range and Fig. 1 show that the reactive power control at the LV level is not very effective.

The low effectivity of reactive power control was utilized for the newly designed control scheme, using the reactive power control primarily for the compensation of injection/consumption of supply point (household) reactive power so this supply point will be self-supporting in regard to reactive power. This control is positioned into the voltage control dead band. Reactive power control is utilized only for significant voltage changes. The reactive power compensation of the supply point decreases the current unbalance of load, thus helping with improving the voltage unbalance in general and reducing active losses. Efficiency is the general rule in distribution and transmission systems operation. Hence every operator tries to diminish active power losses during transmission and distribution across all voltage levels. Based on equations from [8] used for the calculation of power flow and overall losses, current phasors and complex powers for elements connected between node "i" and "j" in a four-wire system can be defined as:

$$\begin{bmatrix} \bar{I}_i^{123n} \\ \bar{I}_j^{123n} \end{bmatrix} = \begin{bmatrix} \bar{Y}_{ii}^{123n} & \bar{Y}_{ij}^{123n} \\ \bar{Y}_{ji}^{abcn} & \bar{Y}_{jj}^{123n} \end{bmatrix} \cdot \begin{bmatrix} \bar{U}_i^{123n} \\ \bar{U}_j^{123n} \end{bmatrix} \tag{6}$$

where $\bar{I}_i^{123n}$ is current phasor in each phase and neutral wire in the node "i" side in A, $\bar{Y}_{ii}^{123n}$, $\bar{Y}_{jj}^{123n}$, $\bar{Y}_{ij}^{123n}$, $\bar{Y}_{ji}^{123n}$ are shunt and series admittances of equivalent Π-element in the four-wire system in S and $\bar{U}_i^{123n}$ is voltage phasor at node "i" in the four-wire system in V. The following equations are the result of complex power expression:

$$\begin{bmatrix} \bar{S}_i^{123n} \\ \bar{S}_j^{123n} \end{bmatrix} = \begin{bmatrix} \bar{U}_i^{123n} \\ \bar{U}_j^{123n} \end{bmatrix} \cdot \begin{bmatrix} \bar{I}_i^{123n} \\ \bar{I}_j^{123n} \end{bmatrix}^* \tag{7}$$

where $\bar{S}_i^{123n}$ is the complex power of a four-wire system in node "i" in VA, $\bar{I}_i^{123n}$ is current phasor in each phase and neutral wire in node "i" side in A and $\bar{U}_i^{123n}$ is voltage phasor at node "i" in the four-wire system in V. Complex losses in the transmission network element can be calculated as a vector sum of complex powers at both element ends:

$$\Delta\bar{S}_{ij}^{123n} = \bar{S}_i^{123n} + \bar{S}_j^{123n} \tag{8}$$

where $\Delta\bar{S}_{ij}^{123n}$ are complex losses in VA. Overall losses are then determined as a sum of power losses of each transmission element. The overall losses in a four-wire network with asymmetrical load need to take into account resistance losses in each phase conductor as well as in neutral conductor [58], [59]. Hence it is clear that the reactive power flow in a four-wire LV network results in undesirable active power losses. Therefore, minimizing reactive power flows in single-phase installations is useful.

B. THE NEWLY DESIGNED CONTROL ALGORITHM FOR SINGLE PHASE INVERTER

The newly proposed algorithm uses a widely set insensitivity band of autonomous control $Q = f(V)$. It embeds the reactive power management function into this insensitivity band. This function, when the voltage is within the control insensitivity band $Q = f(V)$, compensates the reactive power consumption of the load point to zero within the inverter's reactive power control range. This makes the load point and, with the widespread adoption of these inverters, the LV network more independent in terms of reactive power consumption. The limited flow of reactive power through the LV network results in savings in active losses. Compensated reactive power consumption helps to symmetrize the load point. Voltage regulation with a steep ramp thus becomes only a safety brake for the voltage due to lower efficiency at the LV level. Fig. 2 shows the form of autonomous control characteristics and is based on [60].

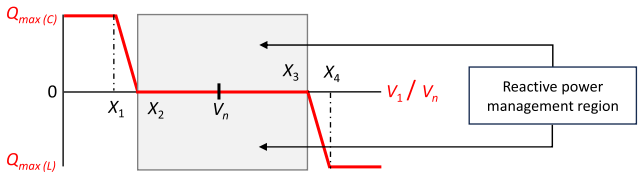

FIGURE 2. Control characteristics $Q = f(V)$ with dead band for reactive power management.

The autonomous control function $Q = f(V)$ can be described by (9):

$$Q(V) = \begin{cases} Q_{max(C)}, & V_1 \le X_1 \\ \dfrac{V_1 - X_2}{X_1 - X_2} Q_{max(C)}, & X_1 < V_1 \le X_2 \\ 0, & X_2 < V_1 \le X_3 \\ \dfrac{V_1 - X_3}{X_4 - X_3} Q_{max(L)}, & X_3 < V_1 \le X_4 \\ Q_{max(L)}, & V_1 > X_4 \end{cases} \tag{9}$$

Points X_1 to X_4 define the characteristics profile and express a dimensionless ratio V_1/V_n. V_1 is measured phase voltage at the inverter's point of connection in p.u. and V_n is the nominal phase voltage of the LV network in p.u. $Q_{max(C)}$ and $Q_{max(L)}$ are the maximum available reactive power for generation and consumption in p.u. [28], [29], [30], [31].

The proposed control algorithm itself is presented in the form of a flowchart in Fig. 3. If the Smart control algorithm is not activated, the inverter operates with zero reactive power. When the Smart control algorithm is activated, the exceeding of the $Q = f(V)$ threshold is checked first. If the threshold is exceeded, predefined autonomous control is activated. If the threshold is not exceeded, the inverter compensates the reactive power of the supply point in the phase it is connected to (and thus regulates to zero the reactive power flow at the interface of the prosumer and DSO). This function is labeled as Reactive power management in Fig. 2 and Fig. 3. In such cases, reactive power measured by the smart meter at the prosumer/DN interface is used as reference input for the compensation control sequence.

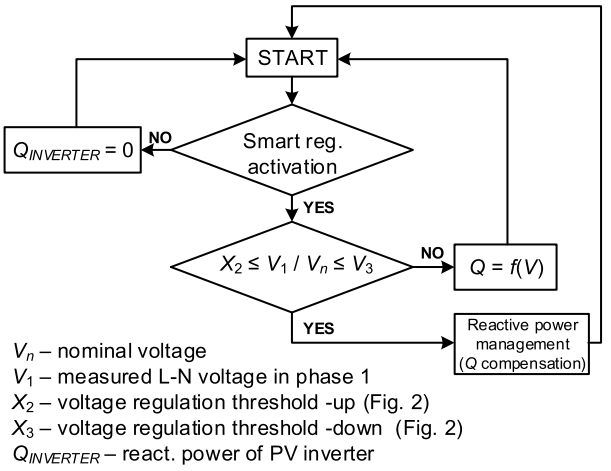

FIGURE 3. The newly proposed single-phase PVP control algorithm characteristics $Q = f(V)$ with dead band for reactive power management.

Measuring data for the inverter needs to be available for the implementation of this algorithm. These data can be transferred from the smart meter through e.g. LAN network [35], [36], [37]. No more data are necessary in the case of autonomous control characteristics since the inverter already has all the data.

A detailed implementation of the proposed control in the control structure of the inverter is shown in Fig. 5 in section III. Compared to the OPF based PV control methods, the undeniable advantage of the proposed method is the zero communication facilities between the individual parts of the network and the absence of central logic. The communication of the inverters with the smart meters is only handled locally within the load points. This ensures the autonomy of the solution, ease of implementation (including financial) and robustness of the solution compared to systems with central logic and extensive communication network.

From the cited references [33], [34], and [35], OPF-based methods can also improve voltage asymmetry in a targeted manner (our proposed algorithm symmetrizes current draw by compensating for reactive power consumption). In order to calculate the voltage asymmetry accurately, the measurement of all the voltage phasors at the point of common coupling, that enter the OPF must be used. However, OPF methods depend on a complex network image (many measurement points) and a reliable communication link with the central logic. This predisposes these systems to high cost and technological complexity compared to stand-alone solutions.

III. IMPLEMENTATION OF THE SMART CONTROL ALGORITHM INTO THE SIMULATED INVERTER CONTROL SYSTEM – THE DYNAMIC SIMULATION

The supply point model with a single-phase PVP and three-phase reactive and active power consumption was created to verify the dynamic behavior of the control algorithm. The dynamic model was created using PSCAD 5.0 [61] with EMTDC calculating core [62]. This model is based on single-phase inverter control using PWM.

Photovoltaic (PV) panels were implemented using the default PSCAD prototype that is based on [63]. A DC-DC converter with hardware designed according to the [64] was connected to these PV panels. The default PSACAD MPPT blocks [65] and [66] were implemented into DC-DC control. Since active power control is not the subject of designed control, DC-DC inverter control used optimized value calculated by the MPPT tracker (the perturb and observe method was used) at the PV panels. DC-DC inverter control was implemented by PWM.

The single-phase inverter uses a full bridge model. Network interference was simulated by an *LCL* filter designed according to the [67]. Inverter control was designed in a d-q-0 system while the PVP control scheme was derived from [68] and [69].

The supply point model utilizes a *RLC* element with set power in each phase. *RLC* values are modeled as constant power consumption [38].

The power line diagram including measured values transmitted through LAN communication (green dotted line) between smart meter and inverter is depicted in Fig. 4.

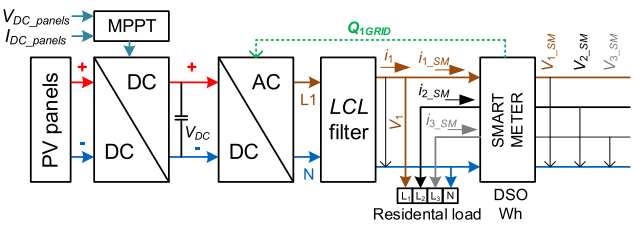

FIGURE 4. Diagram of PVP plant, supply point, and smart meter including the communication link.

The inverter is controlled to a constant voltage by the I_d controller in a DC circuit. The proposed reactive power of Smart control is located in the I_q control implementing

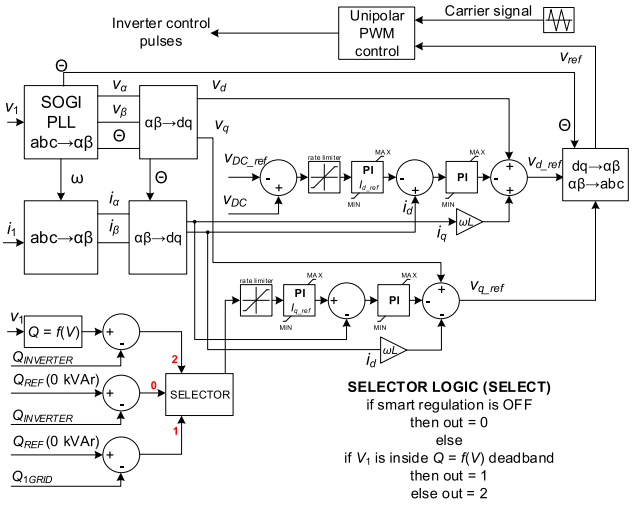

FIGURE 5. Inverter control with implemented Smart control loop (Q_{1GRID} is the reactive power flow measured by the smart meter at the prosumer/DSO interface).

inverter PQ diagram using limiting I_d and I_q values. Fig. 5 depicts the inverter control sequence.

PVP parameterization including the control constants is shown in Table 2.

TABLE 2. Dynamic simulation parameters.

Block	Parameter	Value	Unit
PVP model	PV panels installed power (P_n)	3.27	kW
	Inverter Sizing	4.64	kVA
	Maximal reactive power at P_n	±3.27	kVAr
	Nominal voltage AC (L-N)	0.23	kV
	Nominal frequency	50	Hz
	Nominal voltage DC	0.4	kV
	f_{PWM_AC}	6000	Hz
LCL filter	*L* grid side	1.75	mH
	L inverter side	2.92	mH
	C filter	27.92	μF
	R filter	2.09	Ω
DC-DC boost converter	*L*	23.49	mH
	C	1846	μF
	f_{PWM_DC}	6000	Hz
DC voltage regulator	Proportional Gain	0.1	-
	Integral Constant	0.05	s
Reactive power regulator	Proportional Gain	0.1	-
	Integral Constant	0.5	s

The modeled supply point with PVP was tested using the proposed algorithm to demonstrate the proper operation and effectiveness of the newly designed control. PVP active power and load were constant during the test. Smart control was activated in 0.5 seconds. The PVP supply point was connected to the 1 km line element represented by 240 NAYY cable ($R = 0.125$ Ω/km, $X = 0.08$ Ω/km). A neutral conductor was modeled with the same parameters. The supply point was simulated by 5.4 MVA with $R/X = 0.375$. Function $Q = f(V)$ that new control utilizes was parameterized as follows: $X_1 = 0.9$; $X_2 = 0.92$; $X_3 = 1.08$; $X_4 = 1.1$.

The simulation step for all simulations was set to 10 μs. Fig. 6 shows the results of PVP behavior during simulation including the load time profile. The positive value of power represents the injection of power into the network, negative value represents consumption. Power flows of the supply point (production and consumption together) were monitored using smart meter measurement at the phase the inverter is connected to. The proposed inverter Smart control was activated at the start of the simulation.

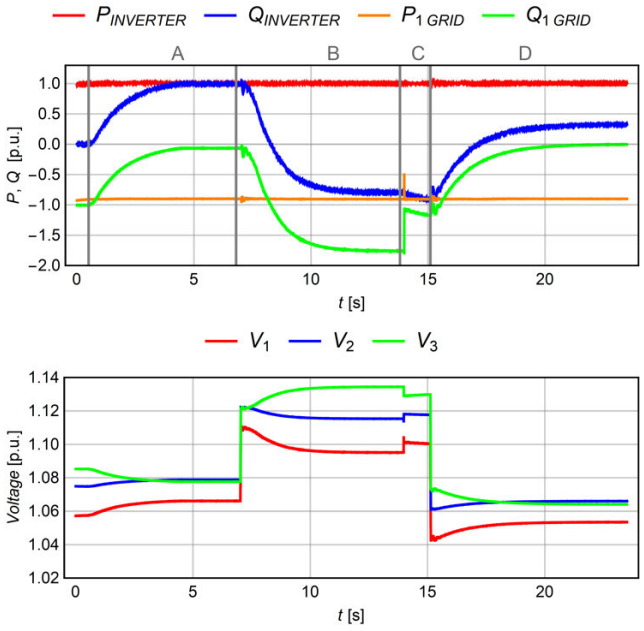

FIGURE 6. Simulation of the response of dynamic model comprising single-phase inverter control (Positive sign for power means power supply to the grid and vice versa), $P_{INVERTER}$ and $Q_{INVERTER}$ are powers at the inverter terminals, P_{1GRID} and Q_{1GRID} are powers measured by smart meter (PVP and consumption together).

In section A of the time profile, inverter-measured voltage was within the dead band. Thus, reactive power management was activated and inverter control has regulated the supply point reactive power consumption to zero. The control reaction time was 5.1 s.

In section B of the time profile, voltage was forced to exceed the $Q = f(V)$ control threshold by simulated network supply. Autonomous $Q = f(V)$ voltage control was activated and the stable working point of inverter's reactive power was achieved while the voltage decreased below 1.1 V_n. Inverter reaction time was 5.5 s while using reactive power control.

In section C, an additional voltage swell was initiated above 1.1 V_n by decreasing reactive power consumption by 0.7 p.u. The inverter increased the reactive power consumed from the network up to the maximum value of -1.0 p.u.

In section D, the step return of voltage to the $Q = f(V)$ dead band was simulated in the inverter point of connection. The reactive power management mode was reactivated and inverter has compensated the supply point reactive power consumption to zero again. The inverter reaction time was 5.3 s in this case.

The dynamic behavior during reactive power control for power plants in a LV network is defined in [5] and [7]. These documents define reactive power control so that the generating module shall reach 90% of the set value in 1–5 s and 100% in 5–60 s. The presented simulation was set for fast dynamic so that required values would be achieved in the shortest possible time in compliance with relevant regulations. The simulation demonstrates easy implementation of the proposed control to the inverter control system while compliance with control time requirements is achieved.

IV. CONTROL BENEFITS CASE STUDY

A case study utilizing the European benchmark LV network (residential feeder) [57] was created to verify the long-term benefits of the proposed control, see Fig. 7. The case study aims to evaluate Smart control in regard to the sustaining voltage in the range of $\pm 10\%$ of V_n, cut the reactive power flow to the network during a one-week period and cut the active power losses expressed by active energy as well as voltage unbalance.

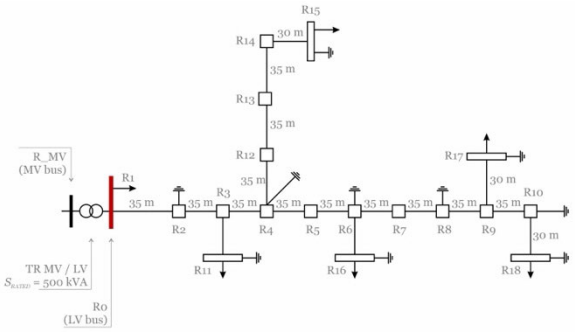

FIGURE 7. LV benchmark network (residential feeder) according to [57].

The simulation model was created in MATLAB/Simulink with the Simscape Electrical module. In the solver, a sample time of 0.5 s was chosen for the calculation of the RMS values. The parameters of short circuit power, transformer, cables and earthing were taken from the default network setup described in the document [57]. The LV lines model uses an exact four-wire diagram through 4 $\times$ 4 matrixes respecting interphase relations, including earthing. Supply points with single-phase connected PVP are modeled in each node. Data from the largest DSO in the Czech Republic was used in the presented simulations. Weekly profiles of active power and reactive power consumption for each phase were created using smart meters aggregated data for each supply point respecting installed power (based on circuit breaker dimension acquired from smart meters data) and Coincidence factors [57]. Thus, the simulation demonstrates a single summer week (from Monday to Sunday) in 15-minute intervals. The unit power of a typical single-phase PVP was selected (3.68 kW). The PVP was always connected to the most loaded supply point phase. A PVP generation profile was created

from solar illumination measurement at the PVP during one week with 15-minute resolution (again data from DSO). PVP distribution to each node is demonstrated in Table 3.

TABLE 3. Number of unit PVP in node and phase.

PVP	L1	L2	L3
R1	5.52 kW (1.5)	5.52 kW (1.5)	14.72 kW (4)
R11	3.68 kW (1)	0 kW (0)	0 kW (0)
R15	1.84 kW (0.5)	3.68 kW (1)	9.2 kW (2.5)
R16	1.84 kW (0.5)	7.36 kW (2)	5.52 kW (1.5)
R17	1.84 kW (0.5)	3.68 kW (1)	1.84 kW (0.5)
R18	3.68 kW (1)	1.84 kW (0.5)	5.52 kW (1.5)

There were two evaluated variants of PVP inverter PQ diagrams; Type A with maximum reactive power range Q/P_n from 0.484 to −0.484 with no Q 24/7 function and Type B with wide reactive power control range from 1 to −1 of Q/P_n with Q24/7 function. The inverter control characteristic setting of $Q = f(V)$ function is in compliance with tagged key points shown in Fig. 2 as follows: $X_1 = 0.93$; $X_2 = 0.95$; $X_3 = 1.08$; $X_4 = 1.1$. Four calculation scenarios were analyzed in the case study:

1) **Scenario 1**: Supply points with consumption only, i.e. no PVP installation in the system.
2) **Scenario 2**: Supply points with consumption and PVP installation, all inverters power factor set to 1.
3) **Scenario 3**: Supply point with consumption and PVP installation, all inverters working with proposed Smart control, PQ diagram does not support Q 24/7 function (Type A PQ diagram).
4) **Scenario 4**: Supply point with consumption and PVP installation, all inverters working with proposed Smart control, PQ diagram supports Q 24/7 function with a wide range of reactive power (Type B PQ diagram).

V. CASE STUDY MAIN RESULTS

A. VOLTAGE MAGNITUDE

Various ways are used to visualize simulation results. The first way contains voltage profiles for each phase and particular nodes during the whole simulation period. As expected, there are significant differences between each node of the modeled network as well as important differences between assessed scenarios. Fig. 8 shows voltages in node R0 at the LV busbar. Minimum voltage variation from the value set at the LV busbar can be seen there.

On the contrary, at the terminal end (e.g. node R18) the voltage variation is way more significant, and a significant range of voltage values is experienced, particularly due to the high short-circuit loop impedance of the relevant node in the network, see Fig. 9. The maximum allowed voltage of 1.1 p.u. is exceeded particularly during the period when the PVP generates the highest active power (typically around noon). A PVP with no $Q = f(V)$ control exceeds the permissible maximum voltage more frequently. The minimum permissible voltage is exceeded mostly during nighttime with more significant active power consumption (e.g. resulting from relevant DSO's power tariff policy). The benefit of Q at night can be seen as well.

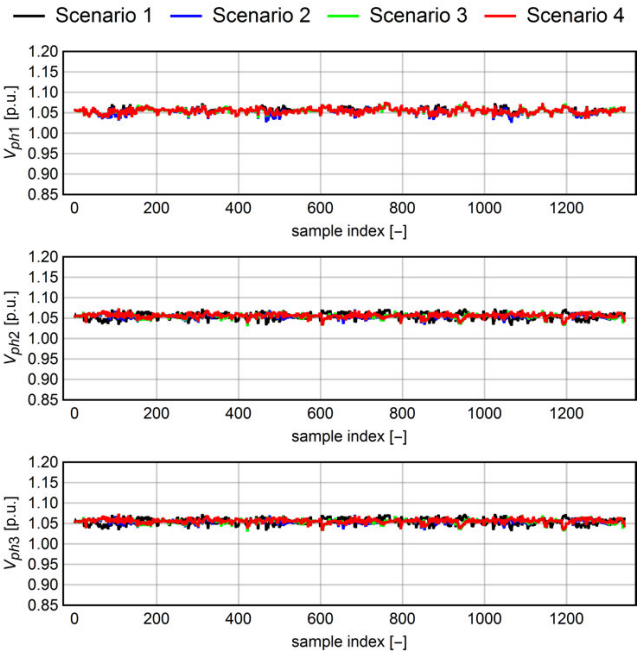

FIGURE 8. Voltage RMS values in the node R0 at the LV busbar.

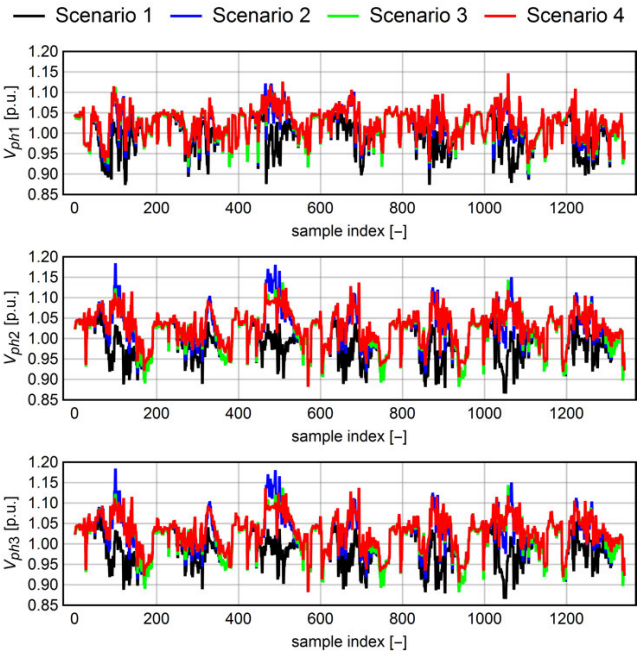

FIGURE 9. Voltage RMS values in the node R18.

The second way of presenting the results is based on statistical evaluation of voltage RMS values in each phase at all nodes. Fig. 10 shows the probability density of results. In almost all cases (nodes and phases), the significant benefit of the $Q = f(V)$ control can be seen, whereas improved Q

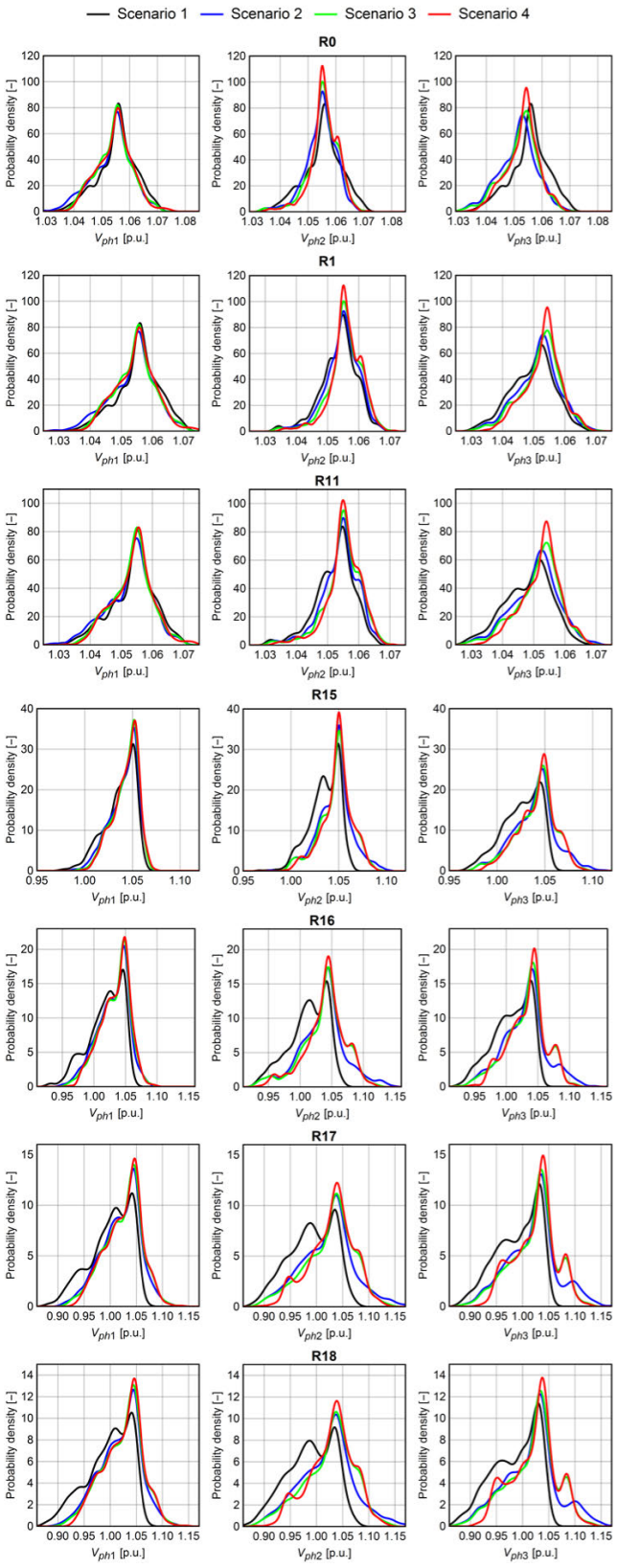

FIGURE 10. The probability density of phase voltages at each node for all evaluated scenarios.

at night (red curve) function produces the best results of all assessed scenarios. This benefit is most significant in the nodes and phases with the highest installed PVP power (according to the Table 3). Particularly in the nodes at the terminal end (R16, R17 and R18), the control ensures that the voltage is almost always within the permissible range of 0.9–1.1 p.u. The benefit is validated by the evaluation of the percentage share of voltage values in the permissible range of 0.9–1.1 p.u., see Table 4.

Table 4 shows to what extent the ratios in the nodes comply with the required voltage range of 0.9–1.1 V_n (EN50160 requires 95% of the number of measurement intervals). Results demonstrate that, in terms of this criterion, the nodes at the end of the terminal are particularly troublesome (nodes R16, R17 and R18).

TABLE 4. Percentage share of voltage values in the permissible range of 0.9–1.1 p.u. for all nodes and scenarios.

Node	Scenario 1	Scenario 2	Scenario 3	Scenario 4
R0	100.0%	100.0%	100.0%	100.0%
R1	100.0%	100.0%	100.0%	100.0%
R11	100.0%	100.0%	100.0%	100.0%
R15	100.0%	99.9%	100.0%	100.0%
R16	100.0%	97.8%	99.3%	99.4%
R17	98.5%	95.7%	97.8%	98.3%

B. VOLTAGE UNBALANCE

The voltage asymmetry factor was determined by transforming the phase voltages at individual nodes into sequence components according to the definition [70] given in [9]:

$$\%VUF = \frac{V_{L-N\_negative}}{V_{L-N\_positive}} \tag{10}$$

where $\%VUF$ is the dimensionless voltage scale of voltage unbalance calculated through voltage sequence components, $V_{L-N\_negative}$ is the negative sequence of voltage in V and $V_{L-N\_positive}$ is the positive sequence of voltage in V. Since the $\%VUF$ indicator is defined through voltage components, the single-phase reactive power control can deteriorate it. While single-phase PVP generates a significant volume of active power while utilizing reactive power regulation $Q = f(V)$, the current phasor in the relevant phase is angle-shifted. Though voltage change can decrease phase voltage variation from average voltage, the $\%VUF$ indicator deteriorates due to the unbalance voltage calculation using phasor magnitudes and angles. This effect can be illustrated using Fig. 11, which shows the voltage unbalance density in each node for one week. This impact is significant during significant PVP generation, particularly when the $Q = f(V)$ control is activated due to the severe voltage variations. In such cases, the deterioration of $\%VUF$ is undesirable collateral damage. On the contrary, reactive power compensation of the supply

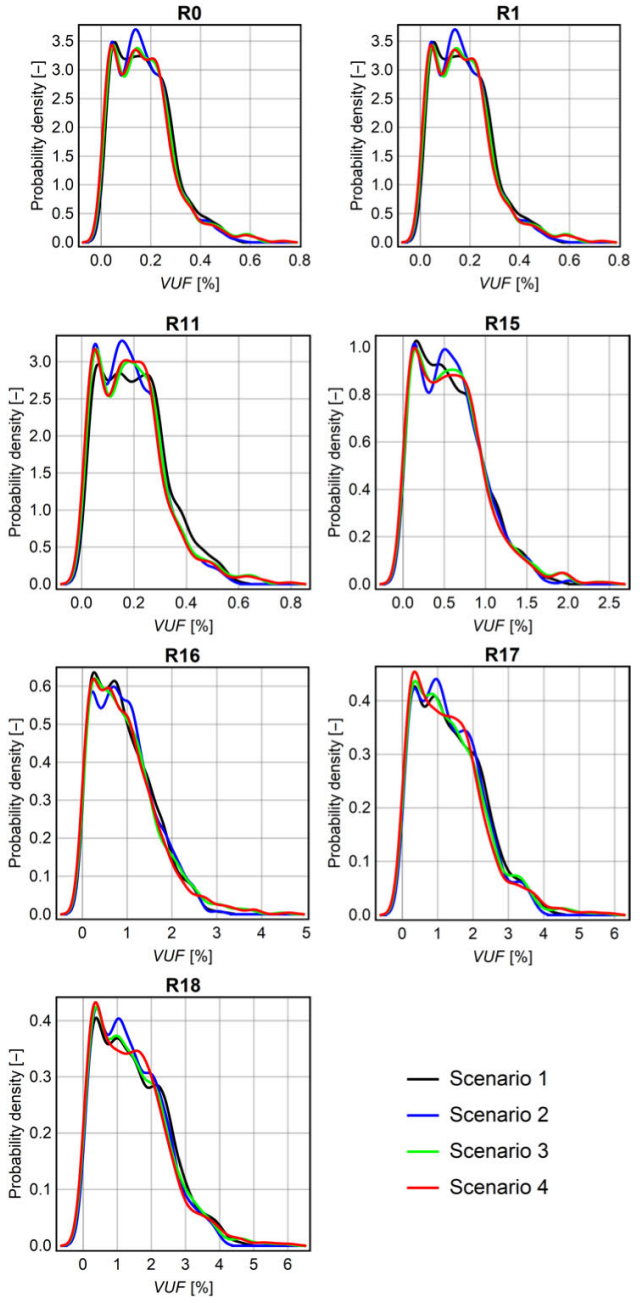

FIGURE 11. The probability density of %VUF at each node for all evaluated scenarios.

point in the dominant phase improves the $\%VUF$ indicator if $Q = f(V)$ control is not activated. Voltage unbalance is improved by reactive power compensation at a given phase, thus the $\%VUF$ indicator is improved as well.

In some cases (for example simple meter), voltage unbalance is determined by a simplified equation from [70]:

$$\Delta\%PVUR = \frac{V_{L-N\_max}}{V_{L-N\_avg}} \tag{11}$$

where $\%PVUR$ is the dimensionless scale of voltage unbalance, ΔV_{L-N_max} is the biggest voltage variation from the average voltage value in V and V_{L-N_avg} is phase voltage, calculated as the algebraic average of three-phase voltages in V. This definition does not consider phasor voltage angles. Better results for the voltage unbalance factor can be obtained using this type of calculation, but these results could be misleading.

C. THE ASSESSMENT OF ACTIVE POWER LOSSES

Active power losses are assessed in regard to the overall losses in the whole LV network, partial losses in the cable network and the whole four-wire LV system, and partial losses at the supply transformer. Losses were calculated for one week of simulation. By comparing each scenario, it is clear that through the installation of a single-phase PVP (shown in Table 5) with no reactive power control, the overall reactive power losses were decreased by 14.5% (local consumption is covered by PVP generation).

TABLE 5. Details of calculated LV network active power losses.

	Scenario 1 [kWh]	Scenario 2 [kWh]	Scenario 3 [kWh]	Scenario 4 [kWh]
Transformer	192.883	192.597	191.980	191.793
LV cables	148.941	99.621	98.823	96.130
Total	341.824	292.218	290.803	287.923

When the newly designed algorithm is applied, an additional 0.5% decrease in active power losses can be achieved in the case of the Type A PQ diagram or a 1.5% decrease in the case of the Type B diagram with Q at night function. A major cut in active power losses was calculated for a four-wire LV network. Therefore, the benefits of newly designed control can be clearly seen in regard to the active power losses.

D. THE ASSESSMENT OF REACTIVE ENERGY

The assessment of LV network reactive energy was made for the supply transformer (primary and secondary side), for reactive power consumption of the supply points and for the PVP inverters (reactive energy for reactive power injection and consumption was calculated specifically). Reactive energy was determined for one whole week of simulation.

Based on the simulation, the integration of the PVP with no reactive power control into the LV network results in small variations of overall reactive energy variation (measured at the primary side of the supply transformer) that are caused by active power flow changes and subsequent voltage change.

When new reactive power control is implemented (Type A PQ diagram – scenario 3), the LV network consumes 39% less reactive energy from the MV network. In the case of the Type B PQ diagram using Q at night function, the reactive power cut in the LV network increased to 64%. The volume of reactive energy that the LV network consumes from the MV network increases with the activation of the $Q = f(V)$ function during peak PVP generation. The $Q = f(V)$ control along with the new controlling algorithm, which utilizes a wide dead band range, saves reactive energy. If the

voltage exceeds the threshold, this function contributes to voltage control within a few percent of the inverter's total reactive energy. The bigger reactive energy consumption of the inverters in scenario 4 results from their wider reactive power control range (Type B PQ diagram).

The volume of reactive energy injected by inverters into the network represents the sum of reactive energy for $Q = f(V)$ control (in case voltage of the inverters is not within the control threshold) and reactive energy injected into the supply point by reactive power management functions. Reactive energy cuts and increased self-sustainability of the LV network in regard to reactive energy using new control are evident, see Table 6.

TABLE 6. Details of calculated LV network reactive power energy.

	Scenario 1 [kVArh]	Scenario 2 [kVArh]	Scenario 3 [kVArh]	Scenario 4 [kVArh]
Transformer MV side	1 180.694	1 138.864	700.036	405.476
Transformer LV side	950.903	926.083	488.533	194.710
Load consumption	882.681	882.681	882.681	882.681
PV inverter injection	–	–	459.520	753.586
PV inverter consumption	–	–	22.326	24.385

E. OPERATIONAL PQ DIAGRAMS OF THE SUPPLY POINT

Control actions and the impact of a specific scenario on the PQ diagram of each node are illustrated in Fig. 12 and Fig. 13. Positive active and reactive power represent the consumption of power from the network; negative active or reactive power represents the injection of power from node to network. Node "R1" was selected because of its high short-circuit power and node "R18" as being the farthest node (electrically) with the lowest short-circuit power.

Fig. 12 and Fig. 13 clearly show that the PVP in a specified installation scheme with no control results in active power overflows from nodes to network (scenario 2). The biggest overflows from nodes to network occur at the dominant phase (phase 3 according to Table 3).

The implementation of a new control results in a PQ diagram change. As can be seen in Fig. 12 and Fig. 13, controls tend to reduce reactive power in every monitor node if the voltage is within the $Q = f(V)$ threshold. The effect is illustrated the best in node "R1" (biggest short-circuit power), where the reactive power in all phases is almost completely compensated using scenario 4 with a wide PQ diagram and Q at night function, hence the node is neutral from a reactive power perspective. In the case of node "R18", the $Q = f(V)$ control threshold is exceeded due to the high impedance and PVP generation. Reactive power management

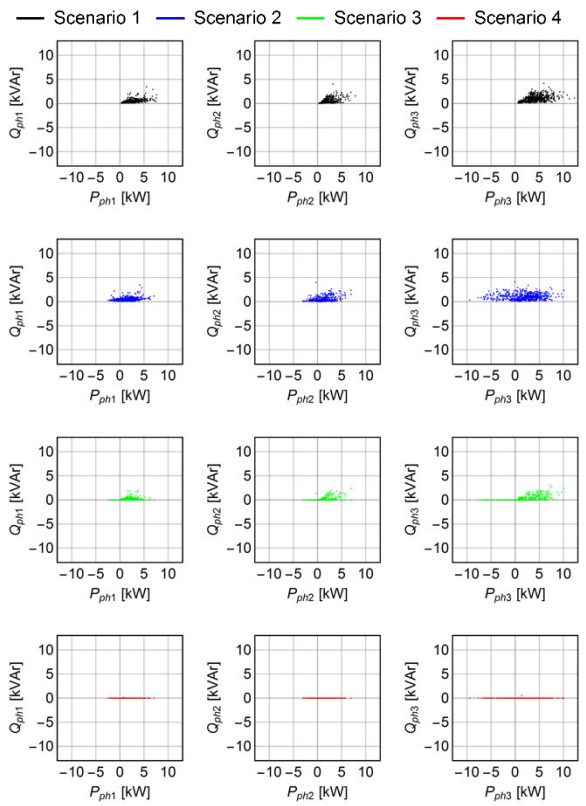

FIGURE 12. Node "R1" PQ diagram, supply point connected to the low impedance network part.

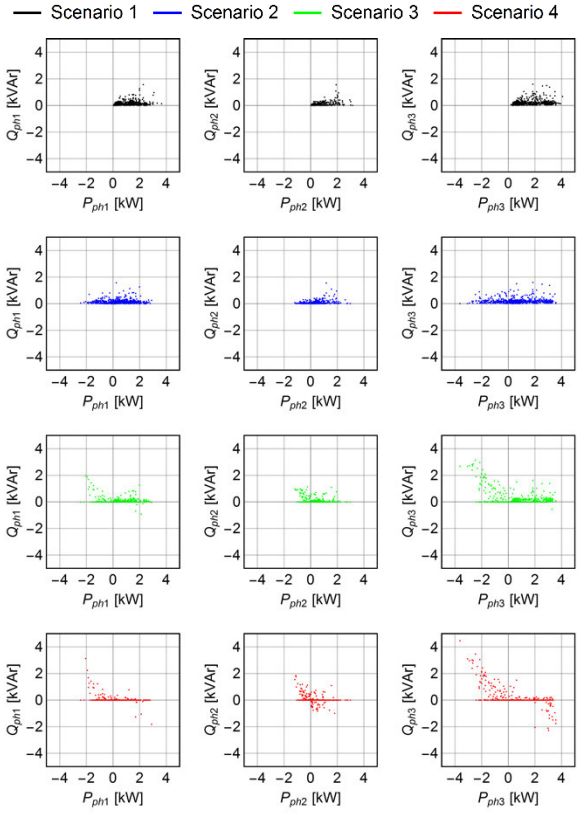

FIGURE 13. Node "R18" PQ diagram, supply point connected to the high impedance network part.

and $Q = f(V)$ control is applied in each phase. Control actions of $Q = f(V)$ consuming reactive power (during peak PVP generation) are evident in scenario 3 with a Type A PQ diagram. Scenario 4 additionally contains evident interventions in reactive power supply with subsequent reactive power overflows from node to network. This is a result of inverter control action with Q at night function during high consumption evening hours when voltage falls under the threshold of $Q = f(V)$ control. PQ diagrams of this node are therefore most similar to the $Q = f(V)$ control characteristic.

VI. CONCLUSION

The paper deals with the planned development of PVP in LV networks and the necessary careful reactive power management. Thus, a new control algorithm for developing a segment of single-phase inverters was created to control supply point reactive power as a whole, decreasing supply point voltage unbalance, to control the voltage at the point of common coupling, and to participate in LV network reactive power control in general.

The dynamic behavior of the new algorithm was tested in PSCAD software, where the voltage control dynamic as well as the dynamic of the compensation mode for reactive power in the supply point comply with requirements defined by RfG [5] and EN 50549-1 [7].

Additionally, the control algorithm was tested under a European benchmark LV network [57] case study with a fully four-wire network model. The benefits of implemented control modes were compared with situations where no PV regulation is available. One control mode used a narrow PQ diagram range, the other used a wide PQ diagram mode (including Q 24/7 function).

Results show the expected impact of $Q = f(V)$ control on minimizing intervals when voltage exceeds the range $\pm 10\%$ of MV even for wide range dead band (control is used in voltage "emergency brake" mode).

Reactive power compensation in the threshold of autonomous $Q = f(V)$ control significantly reduced the reactive power flow in the LV network, which otherwise shall be injected from higher voltage levels. In the case of the Type A PQ diagram, a reduction of 39% of reactive energy was achieved; in the case of the Type B PQ diagram utilizing the Q 24/7 function with a wider Q range, the reduction of 64% of reactive energy was achieved from the summary of 1139 kVArh for one week.

In scenarios with implemented control, active power losses in the LV network were reduced by 0.5% (Type A PQ diagram) and 1.5% (Type B PQ diagram).

Voltage unbalance improvement was experienced in the case of supply point reactive power compensation in the dominant phase. On the contrary, voltage unbalance deteriorates when autonomous $Q = f(V)$ control is active. This is based on voltage unbalance definition [9] that uses voltage positive and negative sequences. If the single-phase inverter activates reactive power control in the voltage change suppression mode, the current phasor in the single phase is angled leading to possible deterioration of voltage unbalance.

Compared with methods described in section I. (part E), the benefit of the new algorithm is that it supports an autonomous solution determined only by the supply point itself. The suggested solution requires neither central logic nor expensive communication links throughout the LV network (as methods based on OPF). This control method can be introduced within existing mandatory inverter support requirements for networks (a defined minimal reactive power range according to legislation) by implementation instruction on the national level.

VII. RECOMMENDATIONS AND FUTURE WORK

In the future, financial incentives for wider reactive power support could be implemented to motivate prosumers for wide reactive power grid support in the best case with Q at night function. Contrary to most other applications, the suggested approach does not use $Q = f(V)$ as primary voltage control but rather as an "emergency brake" while the available dead band is utilized for efficient reactive power control. The paper points out that due to $R/X \gg 1$ at the generation point of common coupling at the LV level, the voltage control using reactive power is not very effective and utilization of such control by single-phase inverters can therefore degrade voltage unbalance, which is calculated from voltage positive and negative sequences. Many published papers contain no definition of how voltage unbalance is calculated, hence the impact of single-phase inverters with $Q = f(V)$ control can be misleading if it is based on a simplified definition. Additionally, presented PQ diagrams of the supply point indicate that with no Q at night function, the inverter will be most probably unable to support the network during high consumption periods (e.g. e-mobility).

Regarding the OLTC application benefits that are published in [25] and [26], we planned to combine the Smart control algorithm with OLTC focusing on both control method coordination. A combined control loop will be created for transformer control, taking LV busbar voltage and voltage in LV network critical point into account.

REFERENCES

[1] *Communication From the Commission to the European Parliament, the European Council, the Council, the European Economic and Social Committee and the Committee of the Regions the European Green Deal*, Eur. Commission, Brussels, Europe, 2019.

[2] G. Strbac, D. Papadaskalopoulos, N. Chrysanthopoulos, A. Estanqueiro, H. Algarvio, F. Lopes, L. de Vries, G. Morales-España, J. Sijm, R. Hernandez-Serna, J. Kiviluoma, and N. Helisto, "Decarbonization of electricity systems in Europe: Market design challenges," *IEEE Power Energy Mag.*, vol. 19, no. 1, pp. 53–63, Jan. 2021, doi: 10.1109/MPE.2020.3033397.

[3] A. Potter, R. Haider, G. Ferro, M. Robba, and A. M. Annaswamy, "A reactive power market for the future grid," *Adv. Appl. Energy*, vol. 9, Jun. 2023, Art. no. 100114.

[4] K. Prochazka, J. Ptacek, P. Bürger, Z. Hruska, P. Filipi, P. Cerny, M. Krátký, and R. Hanus, "Utilization of the reactive power potential in the distribution networks in the Czech Republic," in *Proc. 26th Int. Conf. Exhibition Electr. Distribution*, Sep. 2021, pp. 1460–1464.

[5] *Establishing a Network Code on Requirements for Grid Connection of Generators, EC Regulation*, document EU 2016/631, Brussels, Europe, 2016.
[6] *IEEE Standard for Interconnection and Interoperability of Distributed Energy Resources With Associated Electric Power Systems Interfaces*, Standard IEEE 1547-2018, 2018.
[7] *Requirements for Generating Plants to Be Connected in Parallel With Distribution Networks—Part 1: Connection to a LV Distribution Network—Generating Plants Up to and Including Type B*, document EN 50549-1, Brussels, Europe, 2019.
[8] H. Saadat, *Power Systems Analysis*. New York, NY, USA: McGraw-Hill, 2002.
[9] *Electromagnetic Compatibility (EMC)—Part 3–3: Limits—Limitation of Voltage Changes, Voltage Fluctuations and Flicker in Public Low-voltage Supply Systems, for Equipment With Rated Current ≤16 A Per Phase and Not Subject to Conditional Connection*, Standard IEC 61000-3-3, Int. Electrotechnical Commission, Geneva, Switzerland, 2013.
[10] M. Liu, P. McNamara, R. Shorten, and S. McLoone, "Distributed consensus charging for current unbalance reduction," *IFAC Proc. Volumes*, vol. 47, no. 3, pp. 3146–3151, 2014, doi: 10.3182/20140824-6-za-1003.01943.
[11] S. Helm, I. Hauer, M. Wolter, C. Wenge, S. Balischewski, and P. Komarnicki, "Impact of unbalanced electric vehicle charging on low-voltage grids," in *Proc. IEEE PES Innovative Smart Grid Technologies Europe*, Oct. 2020, pp. 665–669.
[12] R. Stiegler, J. Meyer, M. Höckel, S. Schori, K. Scheida, T. Hanülík, and J. Drápela, "Survey of network impedance in the frequency range 2–9 kHz in public low voltage networks in AT/CH/CZ/GE," in *Proc. 25th Int. Conf. Exhibition Electr. Distrib.*, 2019, p. 5.
[13] H. Zsiborács, A. Vincze, G. Pintér, and N. H. Baranyai, "The accuracy of PV power plant scheduling in Europe: An overview of ENTSO-E countries," *IEEE Access*, vol. 11, pp. 74953–74979, 2023, doi: 10.1109/ACCESS.2023.3297494.
[14] I. Kougias, N. Taylor, G. Kakoulaki, and A. Jäger-Waldau, "The role of photovoltaics for the European green deal and the recovery plan," *Renew. Sustain. Energy Rev.*, vol. 144, Jul. 2021, Art. no. 111017, doi: 10.1016/j.rser.2021.111017.
[15] Eur. Commission. (2020). *Report From the Commission To the European Parliament, the Council, the European Economic and Social Committee and the Committee of the Regions, Renewable Energy Progress Report*. [Online]. Available: https://data.consilium.europa.eu/doc/document/ST-11866-2020-INIT/en/pdf
[16] (2023). *Europe PV Inverter Market—Forecast(2023–2028)*. Accessed: May 9, 2023. [Online]. Available: https://www.industryarc.com/Report/16358/europe-pv-inverter-market.html
[17] Polarismarketresearch. (2023). *Inverter Market Share, Size, Trends, Industry Analysis Report*. Accessed: May 5, 2023. [Online]. Available: https://www.polarismarketresearch.com/industry-analysis/inverter-market
[18] 360marketupdates. (2022). *Global Single-Phase String Inverter Industry Research Report, Growth Trends and Competitive Analysis 2022–2028*. 360 marketupdates. Accessed: May 7, 2023. [Online]. Available: https://www.360marketupdates.com/global-single-phase-string-inverter-industry-21643830
[19] R. Brundlinger. (2019). *Grid Codes in Europe—Overview on the Current Requirements in European Codes and National Interconnection Standards*. [Online]. Available: https://www.researchgate.net/publication/338800967_Grid_Codes_in_Europe_Overview_on_the_current_requirements_in_European_codes_and_national_interconnection_standards
[20] A. Lucas, "Single-phase PV power injection limit due to voltage unbalances applied to an urban reference network using real-time simulation," *Appl. Sci.*, vol. 8, no. 8, p. 1333, Aug. 2018, doi: 10.3390/app8081333.
[21] *Technical Connection Rules for Low-Voltage*, document VDE-AR-N 4100, Germany, 2019.
[22] *Distribution System Operators and Energy Regulatory Office*, Czech grid code for distribution Syst., Prague, Europe, Feb. 2022.
[23] (2023). *Legal Sources on Renewable Energy*. Accessed: May 14, 2023. [Online]. Available: http://www.res-legal.eu/
[24] F. Spertino, A. Ciocia, A. Mazza, M. Nobile, A. Russo, and G. Chicco, "Voltage control in low voltage grids with independent operation of on-load tap changer and distributed photovoltaic inverters," *Electric Power Syst. Res.*, vol. 211, Oct. 2022, Art. no. 108187, doi: 10.1016/j.epsr.2022.108187.
[25] T. Aziz and N. Ketjoy, "Enhancing PV penetration in LV networks using reactive power control and on load tap changer with existing transformers," *IEEE Access*, vol. 6, pp. 2683–2691, 2018, doi: 10.1109/ACCESS.2017.2784840.
[26] A. Arshad and M. Lehtonen, "A stochastic assessment of PV hosting capacity enhancement in distribution network utilizing voltage support techniques," *IEEE Access*, vol. 7, pp. 46461–46471, 2019, doi: 10.1109/ACCESS.2019.2908725.
[27] A. Das, A. Gupta, S. R. Choudhury, and S. Anand, "Adaptive reactive power injection by solar PV inverter to minimize tap changes and line losses," in *Proc. Nat. Power Syst. Conf. (NPSC)*, Bhubaneswar, India, Dec. 2016, pp. 1–6, doi: 10.1109/NPSC.2016.7858955.
[28] E. Demirok, P. C. González, K. H. B. Frederiksen, D. Sera, P. Rodriguez, and R. Teodorescu, "Local reactive power control methods for overvoltage prevention of distributed solar inverters in low-voltage grids," *IEEE J. Photovolt.*, vol. 1, no. 2, pp. 174–182, Oct. 2011, doi: 10.1109/JPHOTOV.2011.2174821.
[29] M. Juamperez, G. Yang, and S. B. Kjær, "Voltage regulation in LV grids by coordinated volt-var control strategies," *J. Modern Power Syst. Clean Energy*, vol. 2, no. 4, pp. 319–328, Dec. 2014, doi: 10.1007/s40565-014-0072-0.
[30] T. O. Olowu, A. Inaolaji, A. Sarwat, and S. Paudyal, "Optimal volt-VAR and volt-watt droop settings of smart inverters," in *Proc. IEEE Green Technol. Conf.*, Apr. 2021, pp. 89–96.
[31] K. Luo and W. Shi, "Comparison of voltage control by inverters for improving the PV penetration in low voltage networks," *IEEE Access*, vol. 8, pp. 161488–161497, 2020.
[32] Y. Z. Gerdroodbari, R. Razzaghi, and F. Shahnia, "Improving voltage regulation and unbalance in distribution networks using peer-to-peer data sharing between single-phase PV inverters," *IEEE Trans. Power Del.*, vol. 37, no. 4, pp. 2629–2639, Aug. 2022, doi: 10.1109/TPWRD.2021.3113011.
[33] F. Nejabatkhah and Y. W. Li, "Flexible unbalanced compensation of three-phase distribution system using single-phase distributed generation inverters," *IEEE Trans. Smart Grid*, vol. 10, no. 2, pp. 1845–1857, Mar. 2019, doi: 10.1109/TSG.2017.2778508.
[34] X. Su, M. A. S. Masoum, and P. J. Wolfs, "Optimal PV inverter reactive power control and real power curtailment to improve performance of unbalanced four-wire LV distribution networks," *IEEE Trans. Sustain. Energy*, vol. 5, no. 3, pp. 967–977, Jul. 2014, doi: 10.1109/TSTE.2014.2313862.
[35] R. Zafar, A. Mahmood, S. Razzaq, W. Ali, U. Naeem, and K. Shehzad, "Prosumer based energy management and sharing in smart grid," *Renew. Sustain. Energy Rev.*, vol. 82, pp. 1675–1684, Feb. 2018, doi: 10.1016/j.rser.2017.07.018.
[36] R. Neal, "The use of AMI meters and solar PV inverters in an advanced Volt/VAr control system on a distribution circuit," in *Proc. IEEE PES T D*, Apr. 2010, pp. 1–4.
[37] M. Manbachi, "Impact of distributed energy resource penetrations on smart grid adaptive energy conservation and optimization solutions," in *Operation of Distributed Energy Resources in Smart Distribution Networks*. New York, NY, USA: Academic, 2018, pp. 101–138.
[38] E. Viciana, F. M. Arrabal-Campos, A. Alcayde, R. Baños, and F. G. Montoya, "All-in-one three-phase smart meter and power quality analyzer with extended IoT capabilities," *Measurement*, vol. 206, Jan. 2023, Art. no. 112309, doi: 10.1016/j.measurement.2022.112309.
[39] J. Yang, W. Tushar, T. K. Saha, M. R. Alam, and Y. Li, "Prosumer-driven voltage regulation via coordinated real and reactive power control," *IEEE Trans. Smart Grid*, vol. 13, no. 2, pp. 1441–1452, Mar. 2022, doi: 10.1109/TSG.2021.3125339.
[40] W. Alabri and D. Jayaweera, "Voltage regulation in unbalanced power distribution systems with residential PV systems," *Int. J. Electr. Power Energy Syst.*, vol. 131, Oct. 2021, Art. no. 107036, doi: 10.1016/j.ijepes.2021.107036.
[41] F. Peprah, S. Gyamfi, E. Effah-Donyina, and M. Amo-Boateng, "Evaluation of reactive power support in solar PV prosumer grid," *E-Prime Adv. Electr. Eng., Electron. Energy*, vol. 2, Jun. 2022, Art. no. 100057, doi: 10.1016/j.prime.2022.100057.
[42] D.-L. Schultis, A. Ilo, and C. Schirmer, "Overall performance evaluation of reactive power control strategies in low voltage grids with high prosumer share," *Electr. Power Syst. Res.*, vol. 168, pp. 336–349, Mar. 2019, doi: 10.1016/j.epsr.2018.12.015.

[43] M. Flota-Bañuelos, M. Espinosa-Trujillo, J. Cruz-Chan, and T. Kamal, "Experimental study of an inverter control for reactive power compensation in a grid-connected solar photovoltaic system using sliding mode control," *Energies*, vol. 16, no. 2, p. 853, Jan. 2023.

[44] V. Kumar and M. Singh, "Reactive power compensation using derated power generation mode of modified P&O algorithm in grid-interfaced PV system," *Renew. Energy*, vol. 178, pp. 108–117, Nov. 2021.

[45] A. Ilo and D.-L. Schultis, "Low-voltage grid behaviour in the presence of concentrated var-sinks and var-compensated customers," *Electr. Power Syst. Res.*, vol. 171, pp. 54–65, Jun. 2019.

[46] A. Momeneh, M. Castilla, J. Miret, P. Martí, and M. Velasco, "Comparative study of reactive power control methods for photovoltaic inverters in low-voltage grids," *IET Renew. Power Gener.*, vol. 10, no. 3, pp. 310–318, Mar. 2016.

[47] D. Almeida, J. Pasupuleti, and J. Ekanayake, "Comparison of reactive power control techniques for solar PV inverters to mitigate voltage rise in low-voltage grids," *Electronics*, vol. 10, no. 13, p. 1569, Jun. 2021.

[48] A. Dhaneria and H. Khambhadiya, "Enhancing the utilization of existing solar inverter by incorporating reactive power compensation feature," in *Proc. Nat. Power Electron. Conf. (NPEC)*, Bhubaneswar, India, Dec. 2021, pp. 1–5, doi: 10.1109/NPEC52100.2021.9672495.

[49] Y. Lavi and J. Apt, "Using PV inverters for voltage support at night can lower grid costs," *Energy Rep.*, vol. 8, pp. 6347–6354, Jun. 2022.

[50] A. Maknouninejad, N. Kutkut, I. Batarseh, and Z. Qu, "Analysis and control of PV inverters operating in VAR mode at night," in *Proc. ISGT*, Anaheim, CA, USA, Jan. 2011, pp. 1–5, doi: 10.1109/ISGT.2011.5759186.

[51] M. Habib, A. Gram, A. Harrag, and Q. Wang, "Optimized management of reactive power reserves of transmission grid-connected photovoltaic plants driven by an IoT solution," *Int. J. Electr. Power Energy Syst.*, vol. 143, Dec. 2022, Art. no. 108455, doi: 10.1016/j.ijepes.2022.108455.

[52] S. Hasan, R. Luthander, and J. de Santiago, "Reactive power control for LV distribution networks voltage management," in *Proc. IEEE PES Innov. Smart Grid Technol. Conf. Eur.*, Sep. 2018, pp. 1–6, doi: 10.1109/ISGTEurope.2018.8571817.

[53] J. Zhou, S. Xu, R. Shao, and L. Chang, "Predictive current controller and compensator-based discrete current controller for single-phase bridge inverters," *J. Power Electron.*, vol. 22, no. 9, pp. 1427–1437, Sep. 2022.

[54] S. Srinivasarangan Rangarajan, J. Sharma, and C. K. Sundarabalan, "Novel exertion of intelligent static compensator based smart inverters for ancillary services in a distribution utility network-review," *Electronics*, vol. 9, no. 4, p. 662, Apr. 2020.

[55] *Voltage Characteristics of Electricity Supplied By Public Electricity Networks*, document EN 50160, 2022.

[56] A. Anurag, Y. Yang, and F. Blaabjerg, "Reliability analysis of single-phase PV inverters with reactive power injection at night considering mission profiles," in *Proc. IEEE Energy Convers. Congr. Expo. (ECCE)*, Montreal, QC, Canada, Sep. 2015, pp. 2132–2139, doi: 10.1109/ECCE.2015.7309961.

[57] S Barsali, *Benchmark Systems for Network Integration of Renewable and Distributed Energy Resources*, document TF C6.04.02, 2014.

[58] W. H. Kersting, "The computation of neutral and dirt currents and power losses," in *Proc. IEEE PES Power Syst. Conf. Expo.*, Sep. 2004, pp. 213–218.

[59] R. M. Ciric, A. P. Feltrin, and L. F. Ochoa, "Power flow in four-wire distribution networks-general approach," *IEEE Trans. Power Syst.*, vol. 18, no. 4, pp. 1283–1290, Nov. 2003, doi: 10.1109/TPWRS.2003.818597.

[60] *Power Generating Plants in the Low Voltage Network*, document VDE-AR-N 4105, 2019.

[61] *Manitoba HVDC Research Centre*, PSCAD, Winnipeg, Canada, 2010.

[62] *EMTDC User's Guide*, Manitoba HVDC Res. Centre, Winnipeg, Canada, 2010.

[63] S. Liu and R. A. Dougal, "Dynamic multi-physics model for solar array," in *Proc. IEEE Power Eng. Soc. Summer Meeting*, Jun. 2002, p. 128, doi: 10.1109/PESS.2002.1043195.

[64] B. K. Perera, S. R. Pulikanti, P. Ciufo, and S. Perera, "Simulation model of a grid-connected single-phase photovoltaic system in PSCAD/EMTDC," in *Proc. IEEE Int. Conf. Power Syst. Technol. (POWERCON)*, Auckland, New Zealand, Oct. 2012, pp. 1–6, doi: 10.1109/POWERCON.2012.6401435.

[65] S. K. Kollimalla and M. K. Mishra, "Variable perturbation size adaptive P&O MPPT algorithm for sudden changes in irradiance," *IEEE Trans. Sustain. Energy*, vol. 5, no. 3, pp. 718–728, Jul. 2014, doi: 10.1109/TSTE.2014.2300162.

[66] K. H. Hussein, "Maximum photovoltaic power tracking: An algorithm for rapidly changing atmospheric conditions," *IEE Proc. Gener., Transmiss. Distrib.*, vol. 142, no. 1, p. 59, 1995, doi: 10.1049/ip-gtd:19951577.

[67] K. A. El Wahid Hamza, H. Linda, and L. Cherif, "LCL filter design with passive damping for photovoltaic grid connected systems," in *Proc. IREC 6th Int. Renew. Energy Congr.*, Jun. 2015, pp. 1–4.

[68] R. Teodorescu, M. Liserre, and P. Rodriguez, *Grid Converters for Photovoltaic and Wind Power Systems*. Piscataway, NJ, USA: IEEE, 2011.

[69] L. Hassaine and M. R. Bengourina, "Control technique for single phase inverter photovoltaic system connected to the grid," *Energy Rep.*, vol. 6, pp. 200–208, Aug. 2020.

[70] R. C. Dugan, *Electrical Power Systems Quality*. New York, NY, USA: McGraw-Hill, 2012.

JOSEF HROUDA received the degree from the Faculty of Power Electrical Engineering, Czech Technical University (CTU), Prague, Czech Republic, in 2012. He is currently pursuing the Ph.D. degree with the University of West Bohemia (UWB), Pilsen, Czech Republic. Since 2012, he has been a Researcher and Developer with EGC—EnerGoConsult ČB s.r.o., České Budějovice, Czech Republic. His research interests include renewable energy sources and their control and modeling of power systems in steady states and transients. He is an active member of the CIRED organization and its working groups.

MARTIN ČERŇAN (Member, IEEE) received the bachelor's degree in applied electrical engineering, the master's degree in electrical power engineering, and the Ph.D. degree in power quality in industrial distribution systems from Czech Technical University in Prague (CTU), Prague, Czech Republic, in 2012, 2014, and 2021, respectively. Since 2014, he has been a Researcher at CTU. His research interests include distribution and transmission system analysis, power quality in industrial distribution systems, and power system reliability. He is a member of IEEE PES.

KAREL PROCHÁZKA received the degree in production and distribution of electrical energy from the Faculty of Electrical Engineering, Czech Technical University in Prague, in 1961, and the Ph.D. degree in production and distribution of electrical energy from Brno University of Technology (BUT), Brno, Czech Republic, in 1972. He joined the Research Institute of Energy, České Budějovice, Czech Republic, where he worked, until 1997. He was mainly engaged in the problematics of the earthing of nodes of MV networks, automation, and protection of MV distribution systems. Since 1997, he has been with EGC—EnerGoConsult ČB s.r.o., where he has been dealing with, among others, the problems of electricity quality and distributed sources. Since 2000, he has also been the main author in the development and modification of the Rules of Operation of Distribution Systems. From 1997 to 2009, he was the Chairperson of the Council of the CIRED in Czech Republic.